

# Effect of Phosphorus on Microstructure and Mechanical Properties of Iron-Based Alloys Processed Through Powder Forging

S. K. Chaurasia<sup>1</sup> · Ujjwal Prakash<sup>1</sup> · Vikram Dabhade<sup>1</sup>

Received: 16 March 2017 / Revised: 5 October 2017 / Accepted: 15 October 2017 / Published online: 6 November 2017  
© Springer Science+Business Media, LLC and ASM International 2017

**Abstract** In sintered as well as cast steels presence of phosphorus is a problem as it induces brittleness in the steels and deteriorates the mechanical properties. The present research work describes a P/M route to produce ductile iron phosphorous alloys. Alloys with phosphorus contents 0, 0.35, 0.65, 1.3, 2, and 3 wt.% were developed by a powder forging route. Care was taken to ensure that no liquid-phase formation takes place during processing. First, a master alloy powder containing 5 wt.% phosphorus was produced by reacting water-atomized iron (Fe) powder with orthophosphoric acid. The iron phosphate (master alloy) particles were then blended with the iron powder. The blended powders were placed in a mild steel can and hot forged at 1323 K in a flowing hydrogen atmosphere. Hot-forged slabs were re-forged to final density and then homogenized at 1373 K for 2 h. Increasing the phosphorus content led to an increase in strength and hardness of forged alloys. Alloys with phosphorus contents < 1 wt.% exhibited significant ductility, suggesting that the presence of phosphorus did not cause the expected embrittlement. The solid-state processing used may lead to development of ductile phosphorus-containing alloys with attractive properties.

**Keywords** Powder forging · Phosphoric iron · Ductility · Mechanical properties · Embrittlement

## Introduction

Phosphorus (P) is an undesirable element in steels. During cold working, phosphorus induces cold shortness or brittleness. Therefore, its content in modern steels is limited to < 0.04 wt.% (all compositions in wt.%). It has been seen that the embrittlement of phosphoric iron is due to segregation of phosphorus along the grain boundaries. The intergranular failure occurs due to the decohesion of grain boundary [1–4]. Phosphorus reduces the resistance of the steel to brittle fracture [5–7]. On the other hand, phosphorus addition has been reported to improve magnetic permeability [8–10] and corrosion resistance [11, 12]. Phosphorus also provides solid solution strengthening to the matrix. Despite these advantages, it is rarely used because of the low ductility associated with phosphorus-containing alloys [13]. Most powder metallurgy (P/M) approaches for Fe–P alloys use liquid-phase sintering by using the eutectic reaction where liquid decomposes into Fe ( $\alpha$ ) and Fe<sub>3</sub>P. In cast alloys, the same reaction takes place in the final stages of solidification. Thus, in cast as well as liquid-phase-sintered P/M alloys the last liquid to solidify at grain boundaries is enriched in phosphorus [14]. In the present work, the Fe–P alloys have been developed by hot powder forging. Care is taken that no liquid-phase formation takes place during processing. Powder forging ensures a higher density and may lead to improved properties [15–17]. In the present work, the powder-forged alloys with phosphorus contents ~ 1 wt.% or less exhibited significant ductility. Possible reasons for this are discussed. The solid-state processing used may lead to development of ductile phosphorus-containing alloys with attractive properties.

✉ S. K. Chaurasia  
skciitr@gmail.com

<sup>1</sup> Department of Metallurgical and Materials Engineering,  
Indian Institute of Technology Roorkee, Roorkee,  
Uttarakhand 247667, India

## Experimental Procedure

A master alloy (Fe–5% P) powder was prepared by mixing distilled water and water-atomized iron powder with orthophosphoric acid ( $\text{H}_3\text{PO}_4$ ). The low carbon (0.01–0.02 wt.%C) water-atomized iron powder was supplied by Hoganas India and had an average particle size of 170  $\mu\text{m}$ . The desired alloy compositions were prepared by blending the Fe powder and the master alloy ( $\text{Fe}_3(\text{PO}_4)_2$ ) in appropriate proportions. Alloys with phosphorus contents 0, 0.35, 0.65, 1.3, 2, and 3 wt.% were prepared. The powders were blended in a laboratory jar mill for 2 h at 400 rpm using 5-mm-diameter steel balls and a 1:5 balls to charge ratio. The blended powder was filled in a cylindrical mild steel can (capsule) of 63.5 mm outer diameter, 2.5 mm wall thickness and 80 mm length. The ends of the can were closed by welding with hemispherical end caps. Two steel tubes of 10 mm diameter and 1 m length were welded to the end caps for passing hydrogen gas. The assembly is shown in (Fig. 1). The filled capsule was kept in a tubular furnace and heated to 1323 K. Hydrogen gas was passed through the tube during heating. After holding for 30 min, the heated powder capsule was removed from the furnace and placed in a channel die for forging in a 100 metric ton friction screw driven forge press. Three to four strokes were given to the hot capsule to form a slab of 20 mm thickness. The slab was then reheated to 1373 K and forged again to 14 mm thickness. The forged slab was homogenized in a muffle furnace at 1373 K for 2 h. The mild steel skin was then removed by machining, and a 10 mm thick plate was obtained. The process has been shown schematically in Fig. 2.

Samples were cut off from the plates for further characterization. Samples measuring  $10 \times 10 \times 10 \text{ mm}^3$  were mechanically polished to one micron grade alumina powder finish and etched using 2% nital solution for examination in an optical microscope and scanning electron microscope (SEM). The grain size of the alloys was measured from optical micrographs using the linear intercept method. The volume percentage of phosphide was measured from polished samples in the optical microscope using a phase analyzer software. X-ray diffraction (XRD) studies were carried out on polished samples in an x-ray

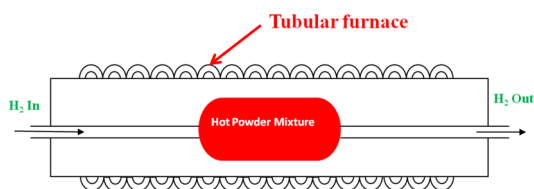


**Fig. 1** Schematic of setup for heating of powder capsule prior to forging

diffractometer. Vicker's hardness measurements were taken on polished sections using a 5-kg load. Tensile test specimens with a gauge length 25 mm and diameter 5 mm were machined from the forged plates as per the ASTM E8M standard. Charpy V-notch Impact test specimens measuring  $10 \times 10 \times 55 \text{ mm}^3$  were machined to form forged plates. All these samples were kept in a muffle furnace at 873 K for 1 h and then furnace cooled to room temperature to relieve the residual stresses. Tensile tests were performed on computer controlled tensile test equipment of 25 kN capacity at a strain  $6.67 \times 10^{-4} \text{ s}^{-1}$ . Charpy impact tests were performed according to ASTM E23 standard. The tensile and impact fracture surfaces were observed by scanning electron microscope. The hardness of matrix and precipitates were measured in a microhardness testing machine on polished samples using a 50 g load.

## Results and Discussion

The forged alloys exhibit iron phosphide ( $\text{Fe}_3\text{P}$ ) precipitates in a ferrite matrix (Fig. 3). Equiaxed grains were observed in all the alloys. Addition of phosphorus results in a decrease in grain size (Table 1). A similar decrease in grain size on phosphorus addition has been reported earlier in cast alloys [18, 19]. Phosphorus partitions were observed between the ferrite matrix and the  $\text{Fe}_3\text{P}$  precipitates (Fig. 4). Line scan in scanning electron microscope shows that phosphorus is distributed within the grains as well as along grain boundaries in the forged alloys (Fig. 5). The scan crosses several grains, but no significant phosphorus

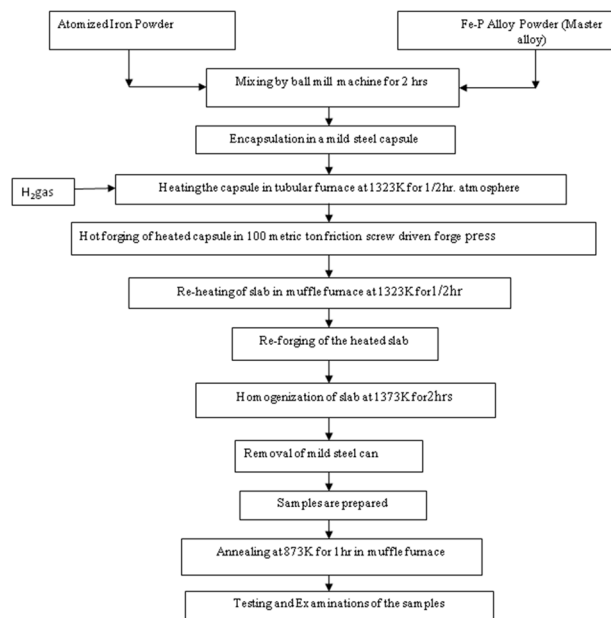


**Fig. 2** Process flowchart of powder forging

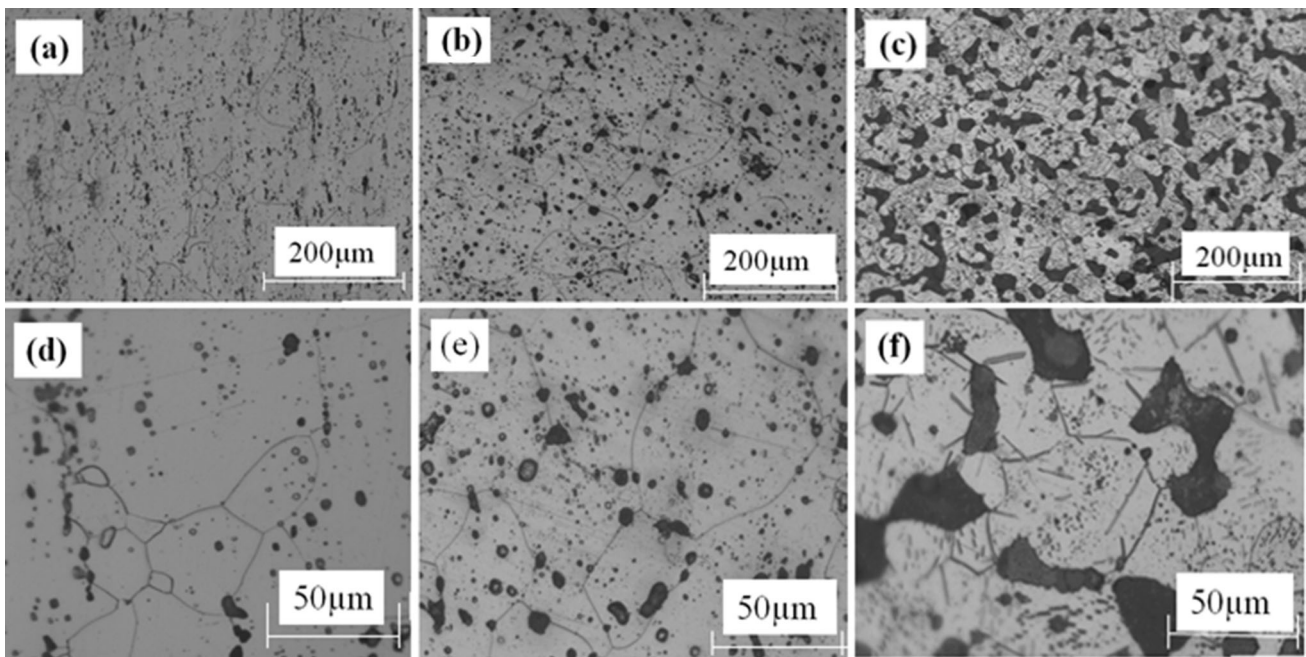


**Fig. 3** Optical micrographs of powder-forged specimens of (a, d) Fe–0.65 wt.%P, (b, e) Fe–2 wt.%P, and (c, f) Fe–3 wt.%P alloy

**Table 1** Grain size and mechanical properties of Fe–P alloys

S. No.	Alloy compositions	Yield stress (MPa)	Total elongation (%)	Hardness ( $H_V$ )	Average grain diameter ( $\mu\text{m}$ )
1.	Fe	$212 \pm 7$	$20 \pm 0.50$	$78 \pm 4$	165
2.	Fe–0.35P	$224 \pm 8$	$17 \pm 0.60$	$95 \pm 6$	155
3.	Fe–0.65P	$260 \pm 6$	$12 \pm 0.50$	$111 \pm 7$	102
4.	Fe–1.3P	$281 \pm 9$	$6 \pm 0.40$	$135 \pm 8$	98
5.	Fe–2P	$351 \pm 6$	$3 \pm 0.20$	$243 \pm 6$	096
6.	Fe–3P	$155 \pm 8$	$2 \pm 0.70$	$125 \pm 5$	092

build up near the grain boundaries could be detected. Tensile test results are shown in Table 1. The tensile strength of the Fe–P alloys increases on the addition of P. This is accompanied by a loss in ductility, particularly in compositions with more than 1%P. This may be because phosphorus addition increases the amount of phosphide in the alloys (Fig. 6), thus reducing ductility at high P levels. The volume fraction of phosphide decides the ductility. Ductility decreases with increasing phosphide volume fraction. The microhardness values of the phosphide phase were similar for all the alloys studied, while the matrix microhardness of the matrix increases with phosphorus content (Table 1) with a maximum at 2 wt.%P. The ferrite matrix is strengthened by the solid solution of phosphorus in iron [20]. In Fe–2%P alloy phosphides are uniformly distributed and are spherical in shape leading to an improvement in strength and hardness [21]. All the alloys were fabricated using same processing conditions. In

particular, the alloy with 3 wt.%P has very high volume fraction of phosphide. These coarse phosphide particles may not be fully densified. The fall in bulk hardness and strength may be related to that [22]. The hardness increased from 78 to 243 Hv with a maximum at 2 wt.%P (Fig. 7). The obtained strength, ductility, and hardness values are better than those reported in the literature [23–25] for alloys with < 1%P. No data have been reported for higher P contents. The theoretical hardness of these alloys was calculated by the following rule of mixtures:

$$H_T \rightarrow f \times H_f + (1 - f)H_m$$

where  $H_T$  theoretical hardness,  $H_f$  hardness of phosphide,  $H_m$  hardness of matrix,  $f$  volume fraction of phosphide.

Figure 7 shows that the theoretical hardness values are greater than the experimental hardness values for all the composition of alloys. The experimental bulk hardness

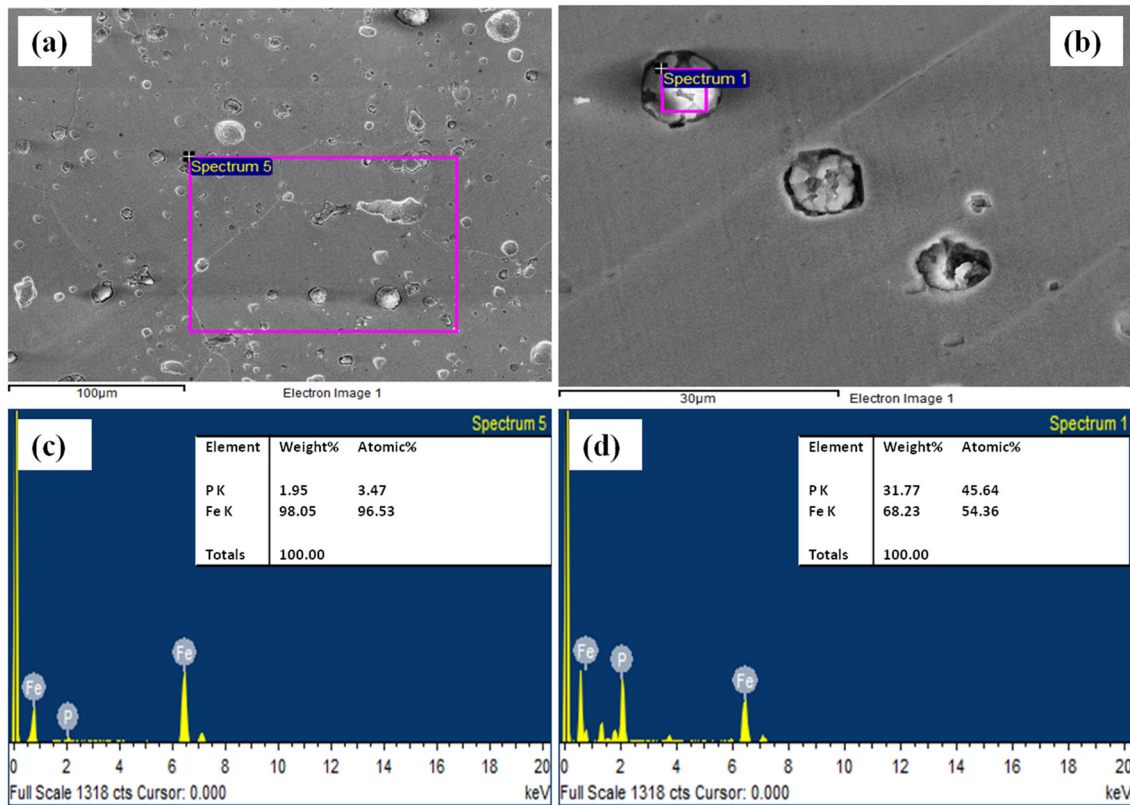


**Fig. 4** (a) Secondary electron scanning electron microscope micrograph of Fe-2 wt.%P alloy. Elemental analysis of matrix (c) and precipitates (d) of Fe-2 wt.%P alloy using energy dispersive analysis of x-rays

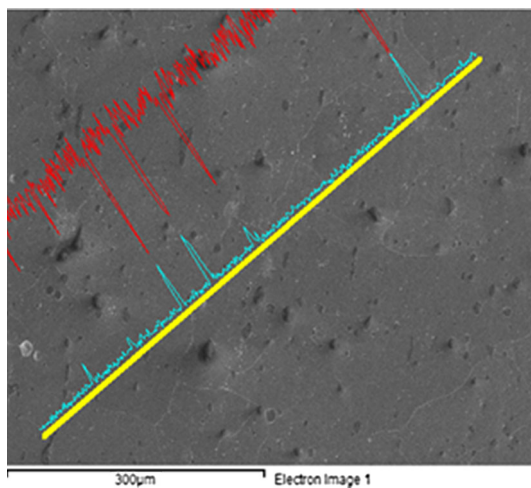


**Fig. 5** Line scan in scanning electron microscope of Fe-0.65 wt.%P showing phosphorus distribution within the grains as well as along grain boundaries in the forged alloys. The blue line is for P, and the red one is for Fe variation. The major peaks indicate the presence of phosphide phase

values are probably more reliable as these cover a larger area than microhardness measurements.

Among P/M processes, powder forging leads to high density and this may explain better ductility observed in the

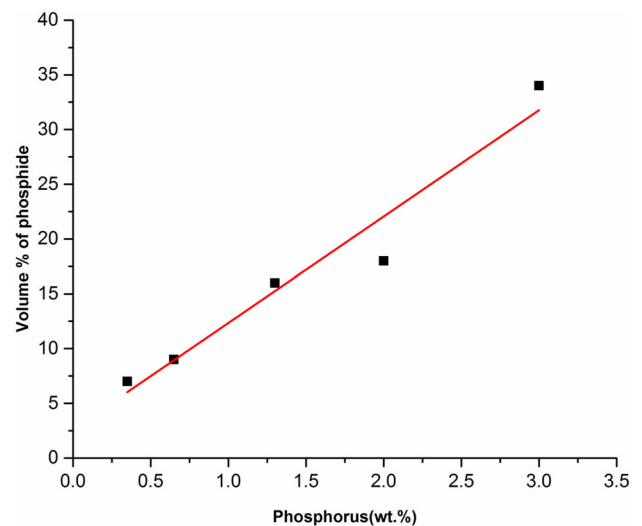


**Fig. 6** Showing volume fraction of phosphide at different phosphorus contents in Fe-P alloys

present research work. Further, chemical and structural homogeneity may also be improved by powder forging [26]. In the casting route, the last liquid to solidify is enriched with phosphorus which is segregated at grain boundaries [27, 28]. This may led to deterioration of

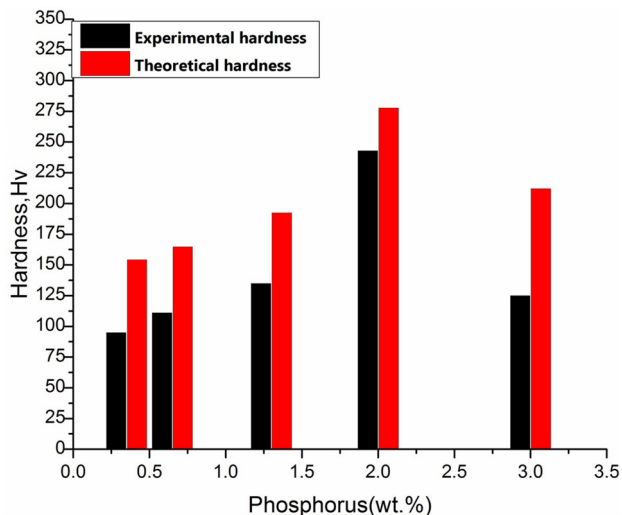


**Fig. 7** Showing theoretical hardness and experimental hardness of Fe–P alloys

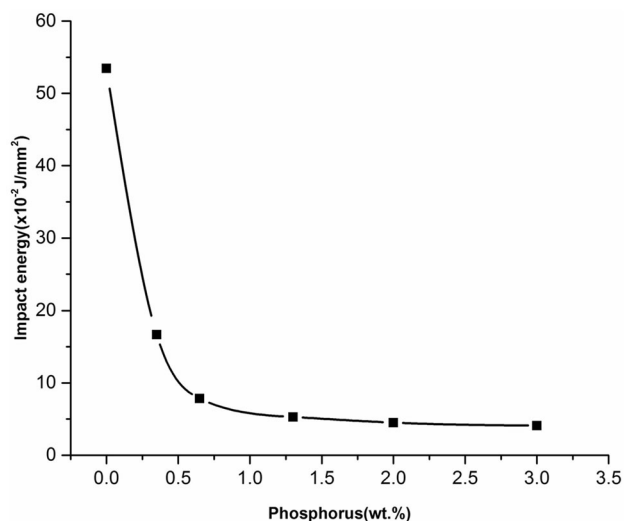


**Fig. 9** Effect of phosphorus on Charpy impact energy of Fe–P P/M alloys

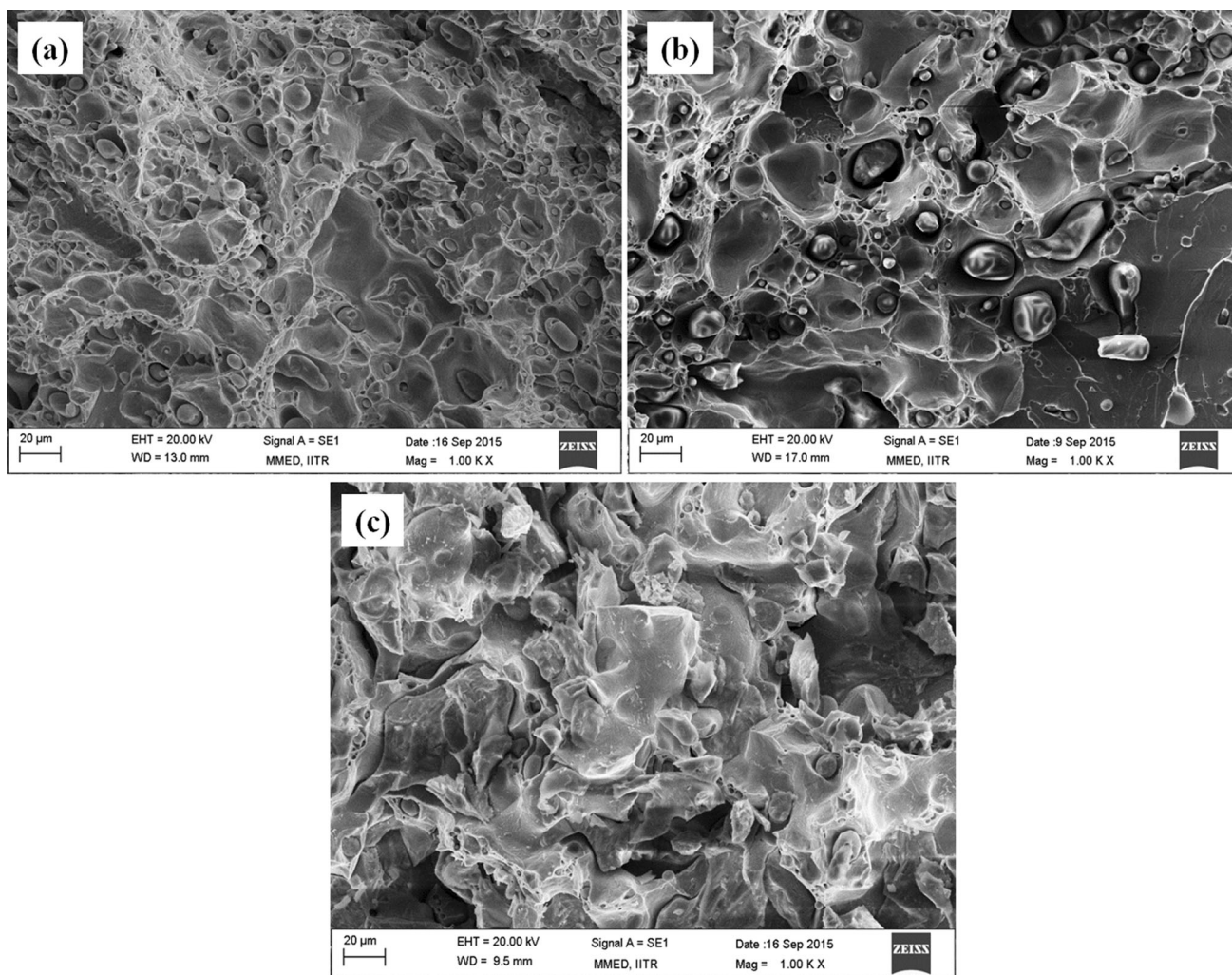


**Fig. 8** Scanning electron microscope micrographs of tensile fracture surfaces of powder-forged specimens (a) Fe–0.65 wt.%P, (b) Fe–2 wt.%P, and (c) Fe–3 wt.%P alloys. (b) shows ductile dimple failure, while

cleavage failure is observed in (c) with Fe–2P alloy showing mixed mode failure

mechanical properties with high phosphorus due to the weakening of grain boundaries [29, 30]. Similarly, P/M routes rely on liquid-phase sintering due to the eutectic reaction where liquid decomposes into Fe ( $\alpha$ ) and Fe<sub>3</sub>P. This also leads to the formation of phosphorus-rich liquid at inter-particle interfaces and consequent phosphorus enrichment at the grain boundaries. Linksdog et al. [31, 32] reported that liquid-phase sintering may be used in P/M Fe–P alloys with phosphorus content up to 0.60% prepared by pressing and sintering route at sintering temperatures above 1323 K. At 1323 K, a Fe–Fe<sub>3</sub>P eutectic results in the formation of a liquid phase which helps to distribute phosphorus in iron by capillary action [8]. This too may lead to phosphorus enrichment at grain boundaries. These

problems in the casting or conventional P/M routes can be overcome by powder forging.

While investigating the effect of phosphorus on magnetic properties of iron it was realized that the Fe–P alloys did not show any cracking during working [33, 34]. Alloys used in the present work have very high phosphorus contents. Though no significant buildup of phosphorus could be detected at the grain boundaries, there are high phosphorus levels present within the grains. There is a gradual loss of ductility with phosphorus content as opposed to embrittlement due to even small amounts of phosphorus (> 0.05%) reported in the literature [27]. The ductility (absence of embrittlement) observed in the present work may be attributed to the absence of liquid phase during

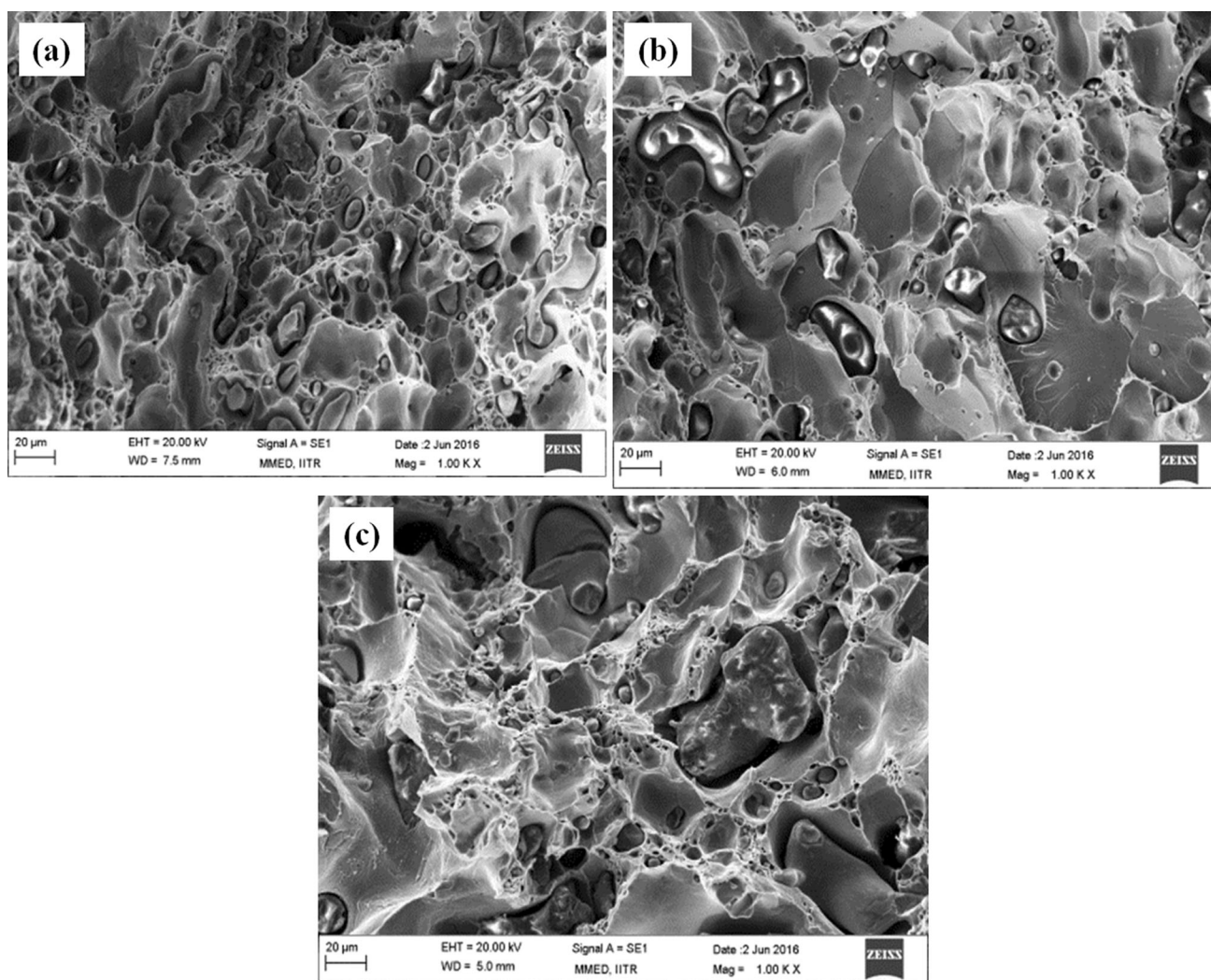


**Fig. 10** Scanning electron microscope micrographs of impact fracture surfaces of powder-forged specimens (a) Fe–0.65 wt.%P, (b) Fe–2 wt.%P, and (c) Fe–3 wt.%P alloys. The alloys with < 1%P exhibit

ductile dimple failure. For the alloys with > 1 wt.%P, the fracture mode is a mix of ductile and cleavage

processing. It is proposed that the presence of phosphorus enriched liquid layer at the grain boundaries is the main cause of embrittlement in conventional steels. Figure 8 shows representative scanning electron microscope micrographs of the fracture surfaces of tensile specimens. Ductile dimple fracture is observed in the low phosphorus alloy, while cleavage failure occurs in the Fe–3%P alloy. Also, a mixed fracture mode may be seen in 2 wt.%P alloy.

Charpy impact results are shown in the Fig. 9. The impact energy decreases with phosphorus content. Though adding P reduces the grain size it also increases the phosphide volume fraction (which is more pronounced) leading to loss in impact values. The Charpy impact fracture surfaces of alloys with < 1%P exhibit ductile dimple failure (Fig. 10). This suggests a greater cohesion, less porosity, and more efficient bonding than that reported [27] during sintering. The use of hydrogen atmosphere during heating of powders may reduce surface oxides and improve interparticle bonding and cleanliness of the P/M part. Further, the coated iron particle surface, i.e.,  $\text{Fe}_3(\text{PO}_4)_2$ , would be transformed to iron phosphide ( $\text{Fe}_3\text{P}$ ), during heating. For the alloys with higher phosphorus content (> 1 wt.%) the fracture mode is a mix of ductile and cleavage. This may be due to the increased volume fraction of the hard and brittle phosphide phase in these alloys.

## Conclusions

1. Ductile Fe–P alloys could be successfully developed using the powder forging route. Use of powder forging overcomes the embrittlement encountered in phosphorus-containing alloys processed through conventional routes.
2. Increasing the phosphorus content in Fe–P alloys increases the strength and hardness. Ductility decreases at high P levels (1% or more) due to large amounts of phosphides in the alloy.
3. Powder forging results in a greater cohesion, less porosity, and more efficient bonding than that reported during sintering. The use of hydrogen atmosphere during heating of powders may reduce surface oxides and improve inter-particle bonding and cleanliness of the P/M part.
4. It is proposed that the solid-state processing route used may overcome the embrittlement encountered during conventional casting as well as liquid-phase sintering routes.

**Acknowledgments** This work was carried out in the Department of Metallurgical and Materials Engineering, IIT Roorkee. MJP Rohilkhand University, Bareilly (UP), India, sponsored one of the authors (S. K. Chaurasia).

## References

1. R. Balasubramaniam, Alloy design of ductile phosphoric iron: ideas from archaeometallurgy. *Bull. Mater. Sci.* **26**(5), 483–491 (2003)
2. K. Abiko, S. Suzuki, H. Kimura, Effect of carbon on the toughness and fracture mode of Fe–P alloys. *Trans. Jpn. Inst. Metals* **23**(2), 43–52 (1982)
3. M. Paju, R. Moller, The effect of boron on phosphorus segregation in austenite. *Scr. Metall.* **18**(8), 813–815 (1984)
4. R. Ding, A. Islam, S. Wu, J. Knott, Effect of phosphorus segregation on fracture properties of two quenched and tempered structural steels. *Mater. Sci. Tech.* **21**(4), 467–475 (2005)
5. V.N. Zikeev, A.P. Gulyaev, V.A. Marchenko, Effect of phosphorus on the properties of structural steels. *Metal Sci. Heat Treat.* **15**(11), 933–935 (1973)
6. V.N. Zikeev, Alloying and the structure of constructional steels resistant to hydrogen embrittlement. *Metal Sci. Heat Treat.* **24**(5), 320–326 (1982)
7. C.L. Briant, Grain boundary segregation of phosphorus in 304L stainless steel. *Metall. Trans. A* **16**(11), 2061–2062 (1985)
8. K.H. Moyer, Magnetic materials and properties for part applications. *ASM Hand Book Powder Metall. Appl.* **7**, 1006–1019 (1998)
9. J.A. Bas, J.A. Calero, M.J. Dougan, Sintered soft magnetic materials. Properties and applications. *J. Magn. Magn. Mater.* **254**, 391–398 (2003)
10. B. Węgliński, J. Kaczmar, Effect of  $\text{Fe}_3\text{P}$  addition on magnetic properties and structure of sintered iron. *Powder Metall.* **23**(4), 210–216 (1980)
11. R. Balasubramaniam, On the corrosion resistance of the Delhi iron pillar. *Corros. Sci.* **42**(12), 2103–2129 (2000)
12. R. Balasubramaniam, Iron pillar. *Current Sci.* **85**(3), 378–382 (2003)
13. G. Straffelini, V. Fontanari, A. Molinari, B. Tesi, Tensile and fatigue behavior of phosphorus alloyed sintered steels. *Powder Metall.* **36**, 135 (1993)
14. J.W. Stewart, J.A. Charles, E.R. Wallach, Iron–phosphorus–carbon system: part 1–Mechanical properties of low carbon iron–phosphorus alloys. *Mater. Sci. Tech.* **16**(3), 275–282 (2000)
15. H.G. Rutz, F.G. Hanejko, High density processing of high-performance ferrous materials, in *International Conference and Exhibition on Powder Metallurgy and Particulate Materials*, Toronto, Canada, (1994)
16. P. Skoglund, M. Kejzerman, I. Hauer, High-density P/M components by high-velocity compaction. *Adv. Powder Metall. Part. Mater.* **4**, 4–85 (2002)
17. E. Klar, P.K. Samal, *Powder Metallurgy Stainless Steels: Processing, Microstructures, and Properties* (ASM International, Materials Park, 2007)
18. B.E. Hopkins, H.R. Tipler, The effect of phosphorus on the tensile and notch-impact properties of high-purity iron and iron-carbon alloys. *J. Iron Steel Inst.* **193**, 218–237 (1958)
19. R. Kirchheim, Grain coarsening inhibited by solute segregation. *Acta Mater.* **50**(2), 413–419 (2002)
20. M.A. Islam, N. Sato, Y. Tomota, Tensile and plane bending fatigue properties of pure iron and iron-phosphorus alloys at room temperature in the air. *Trans. Indian Inst. Met.* **64**(3), 315–320 (2011)
21. E. Klar, M. Svilar, D.F. Berry, Infiltrated powder metal part having improved impact strength tensile strength and dimensional control and method for making same. United States patent US **4**, 861, 373 (1989)
22. F.J. Panetua, J.L. Pereiraa, J.O. Limaa, E.J. Jesusa, L.A. Silvaa, E. Sousa Limab, R.F. Cabrala, C. Santos, Effect of porosity on

- hardness of  $\text{Al}_2\text{O}_3\text{-Y}_3\text{Al}_5\text{O}_{12}$  ceramic composite. *Int. J. Refract. Metals Hard Mater.* **48**, 365–368 (2015)
23. W. F. Jandeska, Strength and ductility enhancement of low temperature sintered iron powder structures. SAE Technical Paper No. 820231 (1982)
  24. T.S. Eyre, Wear mechanisms. *Powder Metall.* **24**(2), 57–63 (1981)
  25. R.V. Batiukov, V.Y. Dorofeev, Z.V. Eremeeva, V.V. Artemov, Preparation of wear-resistant powder materials based on iron by hot stamping in the presence of a liquid phase. *Metallurgist* **55**(3–4), 289 (2011)
  26. W.B. James, M.J. McDermott, A. Robert Powell, Powder forging. *ASM Hand Book Form. Forg.* **14**, 188 (1998)
  27. S.V. Muchnik, Phosphorus-containing sintered alloys (review), *Inst. Mater. Sci.* translated from poroshkovaya Metallurgiya **12**(264), 20–27(1984)
  28. P. Lejcek, *Grain Boundary Segregation in Metals*, vol. 136 (Springer Science & Business Media, Berlin, 2010)
  29. M. Wetzlauffer, R. Kaspar, Effect of phosphorus on the ductility of high strength spring steels. *Steel Res. Int.* **71**(9), 357–361 (2000)
  30. X. Song, Z. Yuan, J. Jia, D. Wang, P. Li, Z. Deng, Effect of phosphorus grain boundaries segregation and precipitations on mechanical properties for Ti-IF steel after recrystallization annealing. *J. Mater. Sci. Technol.* **26**(9), 793–797 (2010)
  31. P. Lindskog, The effect of phosphorus additions on the tensile, fatigue, and impact strength of sintered steels based on sponge iron powder and high-purity atomized iron powder. *Powder Metall.* **16**(32), 374–386 (1973)
  32. P. Lindskog, J. Tengzelius, S. Kvist, Phosphorus as an alloying element in Ferrous P/M. *Mod. Dev. Powder Metall.* **10**, 97–127 (1977)
  33. S.K. Chaurasia, U. Prakash, P.S. Misra, K. Chandra, Development of P/M Fe–P soft magnetic materials. *Bull. Mater. Sci.* **35**, 191 (2012)
  34. S.K. Chaurasia, U. Prakash, K. Chandra, P.S. Misra, Comparisons of sintered technology with powder forging for Fe–P soft magnetic alloys. *Mater. Sci. Forum* **710**, 297 (2012)